THE JOURNAL OF BIOLOGICAL CHEMISTRY
Vol. 278, No. 38, Issue of September 19, pp. 36214–36226, 2003

Printed in U.S.A.

Intra- and Intermolecular Transfers of Protein Radicals in the Reactions of Sperm Whale Myoglobin with Hydrogen Peroxide*

Received for publication, May 6, 2003, and in revised form, July 8, 2003
Published, JBC Papers in Press, July 10, 2003, DOI 10.1074/jbc.M304726200

Olivier M. Lardinois and Paul R. Ortiz de Montellano‡

From the Department of Pharmaceutical Chemistry, University of California, San Francisco, California 94143-2280

Reaction of sperm whale metmyoglobin (SwMb) with H_2O_2 produces a ferryl ($MbFe^{IV}=O$) species and a protein radical and leads to the formation of oligomeric products. The ferryl species is maximally formed with one equivalent of H_2O_2, and the maximum yields of the dimer (28%) and trimer (17%) with 1 or 2 eq. Co-incubation of the SwMb Y151F mutant with native apoSwMb and H_2O_2 produced dimeric products, which requires radical transfer from the nondimerizing Y151F mutant to apoSwMb. Autoreduction of ferryl SwMb to the ferric state is biphasic with t = 3.4 and 25.9 min. An intramolecular autoreduction process is implicated at low protein concentrations, but oligomerization decreases the lifetime of the ferryl species at high protein concentrations. A fraction of the protein remained monomeric. This dimerization-resistant protein was in the ferryl state, but after autoreduction it underwent normal dimerization with H_2O_2. Proteolytic digestion established the presence of both dityrosine and isodityrosine cross-links in the oligomeric proteins, with the isodityrosine links primarily forged by Tyr^{151}-Tyr^{151} coupling. The tyrosine content decreased by 47% in the dimer and 14% in the recovered monomer, but the yields of isodityrosine and dityrosine in the dimer were only 15.2 and 6.8% of the original tyrosine content. Approximately 23% of the lost tyrosines therefore have an alternative but unknown fate. The results clearly demonstrate the concurrence of intra- and intermolecular electron transfer processes involving Mb protein radicals. Intermolecular electron transfers that generate protein radicals on bystander proteins are likely to propagate the cellular damage initiated by the reaction of metalloproteins with H_2O_2.

Protein radicals have been detected in an ever growing number of metalloproteins either as catalytic intermediates, as in cytochrome *c* peroxidase (1), prostaglandin H synthase (2), ribonucleotide reductase (3), pyruvate-formate lyase (4), galactose oxidase (5), and lignin peroxidase (6), or as species that divert oxidizing equivalents away from the normal catalytic pathway, as in prostaglandin H synthase (7), cytochrome *c* (8), cytochrome *c* oxidase (9), cytochrome *c* peroxidase (10), and catalase (11). Protein radical formation has also been extensively studied in the reactions of Mb and hemoglobin with peroxides, both as readily accessible models for the study of such reactions and because these hemoproteins appear to initiate and propagate oxidative damage in various physiological situations (12–18). Protein radicals are commonly generated by the reaction of metal centers with peroxides, but they can also arise by reaction of the proteins with agents such as the hydroxyl radical (19, 20).

Protein radicals, once generated, can participate in catalytic processes or can lead to cross-linking of amino acid residues, covalent bonding of prosthetic groups, formation of protein peroxides, and cleavage of the protein backbone (21). Even the last reactions can be physiologically important, as in the formation of a tyrosine-cross-linked protective shell by sea urchin ovoperoxidase (22), but they are more commonly associated with deleterious biological processes (23). Because of their importance, the formation, localization, delocalization, and propagation of protein free radicals are of intense current interest.

The reactions of metMb[1] with H_2O_2 have provided a useful model for investigation of the general properties of protein radicals. The formation of an EPR-detectable protein radical in the reactions of both SwMb and equine metMb with H_2O_2 is now well established (17, 24). Formation of these protein radicals leads to oligomerization of the metMb monomers. Cross-linking of sperm whale metMb has been found by site-specific mutagenesis in conjunction with protein digestion, peptide sequencing, mass spectrometry, and EPR spectroscopy to involve the formation of Tyr^{103} and Tyr^{151} cross-links (15, 17, 18). Based on the observation of a characteristic fluorescence, these cross-links have been attributed to the formation of dityrosine bonds. Tyr^{146}, the third and last tyrosine in SwMb, forms a radical but does not participate in chemical reactions (18). Evidence exists for additional Mb protein radicals centered on Trp^{14} (18, 24), Cys^{110} (a residue specific to human Mb) (25), and an aliphatic amino acid residue (26).

A ferryl ($Fe^{IV}=O$) species is formed in parallel with formation of the protein radicals in the reaction of metMb with H_2O_2. Although not detected, the reaction of metMb with H_2O_2 may first produce a transient Compound I-like intermediate in which the ferryl species is associated with a porphyrin rather than protein radical (27, 28). Electron transfer from the protein to the porphyrin radical cation would then produce the observed protein radical. The protein residue that provides the electron that quenches the porphyrin radical cation has not been unambiguously identified, but the unpaired electron density readily translocates to residues such as Tyr^{151} and Trp^{14} that are some distance away from the heme group. The Tyr^{151} radical is formed even when the Tyr^{146} and Tyr^{103} residues, which are closer to the heme, have been mutated to phenylala-

* This work was supported by National Institutes of Health Grant GM32488. The costs of publication of this article were defrayed in part by the payment of page charges. This article must therefore be hereby marked "*advertisement*" in accordance with 18 U.S.C. Section 1734 solely to indicate this fact.

‡ To whom correspondence should be addressed: University of California, 600 16th St., San Francisco, CA 94143-2280. Tel.: 415-476-2903; Fax: 415-502-4728 or 415-476-0688; E-mail: ortiz@cgl.ucsf.edu

[1] The abbreviations used are: metMb, metmyoglobin; SwMb, sperm whale metmyoglobin; Mb, myoglobin; LPO, lactoperoxidase; heme, iron protoporphyrin IX regardless of the oxidation and ligation states; EPR, electron paramagnetic resonance; HPLC, high pressure liquid chromatography; FPLC, fast protein liquid chromatography.

nines. A tyrosine-linked pathway for translocation of the protein radical thus does not appear to be required.

Lactoperoxidase (LPO) reacts with H_2O_2 to form a Compound I species with an Fe^{IV}=O ferryl species and a porphyrin radical cation (29). As proposed for Mb, this Compound I intermediate decays to a second "Compound I" species that retains the Fe^{IV}=O but now has a protein rather than porphyrin radical (30, 31). Formation of this second Compound I structure results in dimerization of LPO via a dityrosine cross-link involving Tyr^{289} (32). However, unpaired electron density is shown by spin trapping and EPR studies to reside at sites in addition to Tyr^{289} (32). It is not known whether the protein radicals formed in the LPO catalytic cycle have a biological function other than their probable involvement in autocatalytic covalent attachment of the prosthetic heme group to the protein (33), but we recently provided evidence that the LPO radical can be transferred to metMb (34).

In the present study, we have examined in greater detail the protein radicals formed in the reaction of SwMb with H_2O_2 in order to quantitatively evaluate their fate and to determine the extent to which the protein radical undergoes intra- and intermolecular transfer from one site to another. The translocation of a radical within a protein and within proteins in a common environment is of considerable interest, since it enables the propagation of unpaired electron density from the site of its formation in a metalloprotein to sites that may differ in properties, reactivity, and cellular location.

EXPERIMENTAL PROCEDURES

Materials—SwMb type II acquired from Sigma was used without further purification (this product is no longer commercially available). A stock solution was prepared daily. In some experiments, Mb solutions were purified before use by passage through a Superdex 75 HR gel filtration column (Amersham Biosciences) as described below; identical results were obtained with both the commercial and purified materials. The SwMb concentration was determined from the Soret maximum at 409 nm ($\epsilon_{metMb,409}$ = 157 mM^{-1} cm^{-1}) (35), whereas that of apoMb was determined from the aromatic amino acid band at 280 nm (ϵ_{280} = 16 mM^{-1} cm^{-1}) (36). All aqueous solutions were prepared using water passed through a Milli Q system (Millipore Corp.) equipped with a 0.2-μm pore size filter. Diluted H_2O_2 solutions, obtained from a 30% solution (Sigma), were used within 1 h of preparation. The H_2O_2 concentration was confirmed by absorbance measurements at 240 nm ($\epsilon_{H_2O_2,240}$ = 39.4 M^{-1} cm^{-1}) (37). Leucine aminopeptidase (type IV-S, from porcine kidney microsomes), carboxypeptidase Y (from bakers' yeast), and endopeptidase (protease type X, from *Bacillus thermoproteolyticus* rokko) were from Sigma. Prepacked Sephadex G-25 (PD-10) gel filtration cartridges were purchased from Amersham Biosciences. All other chemicals were of analytical grade and were purchased from Sigma or Roche Applied Science.

Analytical Methods—Absorption spectra were recorded on a Cary 1E UV-visible spectrometer (Varian, Victoria, Australia). Fluorescence excitation and emission spectra were measured with a PerkinElmer Life Sciences LS 50 B fluorimeter (Beaconsfield, UK). The kinetic data for the reduction of ferryl Mb were obtained using a Hewlett Packard 8452A UV-visible diode array spectrometer (Palo Alto, CA). High pressure liquid chromatography (HPLC) was carried out on a Hewlett Packard 1090 liquid chromatography system. SDS-PAGE was done on an Amersham Biosciences Phast System. Gel filtration and ion exchange chromatographies were performed on a fast protein liquid chromatography (FPLC) system.

Preparation and Expression of Site-directed Mutants—The mutant SwMb proteins were expressed, purified, and oxidized to the met form as described previously (17, 34). The far UV circular dichroism spectra of wild-type and mutant SwMb proteins at pH 6.8 were fully superimposable (data not shown). In all mutants examined, the observed UV-visible spectra were nearly identical to those of the native protein, indicating that changes to the structure in the vicinity of the heme iron were minimal (data not shown).

Preparation of ApoMb—ApoMb was prepared by 2-butanone extraction of acidified solutions of SwMb (16). A solution of 50 mg of SwMb in 1500 μl of water cooled to 4 °C was acidified to pH 2.5 by the addition of concentrated HCl. The resulting mixture was extracted with 4 volumes of cold 2-butanone. The organic layer containing the extracted heme was discarded. The aqueous solution was passed over a PD-10 column previously equilibrated and eluted with water. The colored band was collected and loaded directly on a (2.6 × 100 cm) Sephacryl S-200 HR column (Amersham Biosciences). The column was equilibrated and run at 0.50 ml/min in 50 mM potassium phosphate buffer, pH 6.8. The apoprotein eluted as a single symmetric peak that was collected and stored at 4 °C for subsequent analysis. The residual heme content was lower than 1% as evaluated by the ratio of the absorbances at 280 and 408 nm.

Reconstitution of ApoMb with Protoheme—A 1-mg sample of hemin (Aldrich) was dissolved in 1 ml of 0.01 NaOH. The pH was adjusted to 6.8 with 0.1 M HCl, and the hemin was then passed through a 0.2-μm filter to remove the precipitate. 1.5–2 eq of dissolved hemin was added to 3.5 μM apoMb in 50 mM potassium phosphate buffer, pH 6.8, and the mixture was left to equilibrate at room temperature for 2 h. Excess hemin was removed by passage through a PD-10 column previously equilibrated and eluted with 50 mM potassium phosphate buffer, pH 6.8. The colored band of hemin-reconstituted SwMb was collected and stored at 4 °C for subsequent analysis.

Preparation of Dityrosine and Isodityrosine Standards—Dityrosine and isodityrosine were prepared using a combination of published procedures (38, 39). A 4.0-g sample of L-tyrosine was dissolved in 100 ml of 8.5 M NH_4OH, and 10 ml of 0.75 M $K_3Fe(CN)_6$ was added with stirring. The reaction was allowed to proceed for 3 h at room temperature. The reaction was terminated by the addition of 400 ml of isopropyl alcohol, and the mixture was left standing overnight. Centrifugation at 15,000 × *g* for 15 min yielded a clear yellowish brown supernatant. The supernatant was applied on a DEAE-cellulose (Sigma) column (2.5 × 25 cm) previously equilibrated with a mixture of isopropyl alcohol plus 8.5 M NH_4OH (4:1, v/v), and the column was washed with 1 liter of the same solvent mixture. The column was then washed and eluted with 2 M NH_4OH at a flow rate of 15 ml/h. Fractions of 10 ml were collected and evaluated spectrophotometrically at 280 nm. Samples of the major peak were pooled and concentrated to 50 ml in a rotary evaporator under vacuum before adjusting the pH to 8.0 with concentrated NaOH. The resulting solution was then subjected to FPLC on an Amersham Biosciences Mono Q HR 5/5 column previously equilibrated with 10 mM Tris base, pH 8.0. Amino acids were eluted from the anion exchange column with a 26-ml linear gradient of 0–150 mM NaCl in 10 mM Tris base, pH 8.0, at a flow rate of 2 ml/min. Dityrosine and isodityrosine eluted from the anion exchange column in the void volume and at 100 mM NaCl, respectively. The collected peaks were acidified to pH 2.0 by adding concentrated HCl and were then desalted using C18 Sep-Pak cartridges (Waters) previously equilibrated with 0.1% trifluoroacetic acid in water. The cartridges were eluted with 0.1% trifluoroacetic acid in water/acetonitrile (6:4, v/v). Acetonitrile and trifluoroacetic acid were removed under vacuum using a SpeedVac concentrator. The resulting solution was then subjected to FPLC on an Amersham Biosciences Mono S HR 5/5 column previously equilibrated with 10 mM acetic acid, pH 3.0. Amino acids were eluted from the cation exchange column with an 80-ml linear gradient of 0–80 mM NaCl in 10 mM acetic acid, pH 3.0, at a flow rate of 2 ml/min. Dityrosine and isodityrosine eluted from the cation exchange column at 40 and 45 mM NaCl, respectively. The two peaks were desalted as above. After one passage through the Mono Q and the Mono S columns, the oxidation products were apparently homogeneous as assessed by reverse phase HPLC. Each compound eluted as a single symmetrical peak.

Determination of the Extinction Coefficient of Tyrosine Radical Addition Products—The extinction coefficients of tyrosine radical addition products were determined using 2,4,6-trinitrobenzene-1-sulfonic acid for free amino group quantification (40) with calibration on a tyrosine solution. The values obtained by this approach for dityrosine and isodityrosine in 0.1 M NaOH were 8600 M^{-1} cm^{-1} at 316 nm and 5961 M^{-1} cm^{-1} at 296 nm, respectively.

Titration of SwMb with H_2O_2—Titration experiments were carried out at 4 °C in 50 mM potassium phosphate buffer, pH 8.0. Suitable volumes of H_2O_2 solution were added stepwise to a freshly prepared SwMb solution (250 μM), and the spectrum was recorded <6 s after the addition of H_2O_2. After each addition of H_2O_2, a 64-μl aliquot of the incubation mixture was removed and rapidly mixed with 336 μl of a quenching solution composed of 19 mM sodium ascorbate and 84 units of catalase in 50 mM potassium phosphate buffer, pH 6.8. Control experiments (not shown) showed that under these conditions, the ferryl Mb was completely converted to metMb within 1 min. The resulting solutions were stored at 4 °C until they were subjected to FPLC on a gel filtration column as described below to check the progress of the reaction and the nature of cross-linked products.

Correlation of the Autoreduction of Ferryl Mb to MetMb with Oligomerization Yields—Reactions were conducted in 50 mM potassium phosphate buffer, pH 6.8, at 25 °C using 250 μM SwMb stock solutions. The reaction was initiated by the addition of 2.4 eq of H_2O_2. After a 10-s incubation, the excess H_2O_2 was removed by adding catalase (26 units). At various times, a scan was taken, and a 64-μl aliquot of the reaction mixture was removed and rapidly mixed with the ascorbate-catalase solution as above. The resulting solutions were analyzed by FPLC on a gel filtration column to check the progress of the reaction as described below. Pseudo-first-order rate constants for the reaction were calculated by nonlinear regression analysis (the Levenberg-Marquardt algorithm).

Dependence of the Oligomerization Yield on the [Mb]/[H_2O_2] Ratio—SwMb stock solutions (40–2560 μM) were prepared in 50 mM potassium phosphate buffer, pH 6.8, and incubated at 25 °C. Suitable volumes of H_2O_2 solution were added to SwMb to give the desired H_2O_2/SwMb molar ratio. After a 5-min incubation, the excess H_2O_2 was removed by adding catalase (52 units). The resulting solutions were incubated at 25 °C for 2 h and allowed to stand at 4 °C until subjected to FPLC on a gel filtration column as described below.

SDS-PAGE of Protein Samples—Cross-linking experiments were similarly performed in 50 mM potassium phosphate buffer, pH 6.8, at 25 °C for 5 min. The reactions were terminated by the addition of the SDS-PAGE sample buffer. Samples were allowed to stand in SDS for 10 min and heated at 100 °C for 2 min prior to loading onto the gels, which were developed and then stained with Coomassie Brilliant Blue.

Separation and Quantification of SwMb Cross-linking Products by Gel Filtration Chromatography—Samples were diluted to a final concentration of 40 μM in heme and subjected to FPLC on a Superdex 75 HR 10/30 column with detection at 280 nm. The column was equilibrated and run at 0.50 ml/min in 50 mM potassium phosphate buffer, pH 6.8. The yield of cross-linked protein was estimated by comparing the area of earlier eluting peaks (high molecular mass) with that of the peak area obtained for metMb before the addition of H_2O_2. Control experiments (not shown) established that the total area of the peaks at 280 nm remained unaffected by the polymerization. Since the extinction coefficient of the native form and the degree of polymerization of the cross-linked products were known, it was possible to determine the molar concentration of the products. The relative amounts of cross-linked products were calculated by deconvolution of the FPLC traces using the software Origin™ from Microcal Software, Inc. (Northampton, MA). The deconvolution method relies on curve-fitting the chromatograph with *a priori* specification of the number of Gaussian peaks contained in the data.

Reverse Phase HPLC Analysis of the Cross-linked Heme Species—The reverse-phase HPLC analysis of the cross-linked heme species was adapted from the method of LeBrun *et al.* (41). Samples were diluted to a final concentration of 20 μM in heme and were analyzed on a Poros R2, 4.6 × 100-mm, perfusive particule column from Perceptive Biosystems (Framingham, MA). The mobile phase consisted of a mixture of solvent A (0.1% trifluoroacetic acid in water) and solvent B (0.05% trifluoroacetic acid in acetonitrile), and the column was eluted at a flow rate of 1.5 ml/min. The bound and unbound heme species were separated with a linear stepwise gradient of 30% solvent B for 3 min, 30–50% solvent B from 9.5 to 13 min, and 95% solvent B from 13 to 18 min and then adjusted back to 30% solvent B for 2 min. The free heme eluted at 6.0 min and oxidatively modified polar hemes at 2.8 and 3.2 min and the bound heme at around 7.5 min. The heme group and the protein were monitored at 400 and 214 nm, respectively.

Enzymatic Digestion of Monomeric and Oligomeric Forms of SwMb—Since acid and alkaline hydrolysis destroy Trp and some Trp and Tyr derivatives, proteases were used to digest the monomeric and oligomeric forms of SwMb. The enzymatic digestion was adapted from the method of Garner *et al.* (42). A 750 μM SwMb stock solution in 50 mM potassium phosphate buffer, pH 6.8, was incubated with 1.0 eq of H_2O_2 for 1 min at 25 °C. The resulting mixture was subjected to FPLC on a Superdex 75 HR 10/30 column, as described above. The fractions corresponding to monomeric and dimeric forms of SwMb (as assessed by SDS-PAGE analysis) were pooled in two lots. Each lot was desalted over prepacked Sephadex G-25 (PD 10; Amersham Biosciences) gel filtration cartridges and was concentrated to 125 μM by ultrafiltration (Centricon YM 10; Amicon; molecular weight cut-off = 10,000). A 400-μl sample of each concentrated fraction was taken for analysis. After adjustment to pH 8.5, protease type X was added to a final protein/protein ratio of 1:10 (w/w), and the mixture was incubated at 37 °C for 4 h. This step was followed by a treatment at pH 5.2 with carboxypeptidase Y (1:10, w/w) for 8 h at 30 °C and a further treatment at pH 7.2 with leucine aminopeptidase (1:10, w/w) for 8 h at 25 °C. The reactions were stopped by injecting the final mixtures directly onto a reverse phase HPLC column.

Reverse Phase HPLC Analysis of SwMb Proteolytic Hydrolysates—Dityrosine and isodityrosine standards or SwMb hydrolysate samples were injected onto a Vydac 218TP54, 4.6 × 250-mm, C18 reverse phase HPLC column. The column was eluted at a flow rate of 0.8 ml/min with a linear gradient rising from 100% solvent A to 10% solvent B in 45 min: solvent A, 0.1% trifluoroacetic acid in water; solvent B, 0.085% trifluoroacetic acid in acetonitrile. A rapid gradient to 90% solvent B and then back to 100% solvent A was then run in order to regenerate the column. The eluent was monitored with a UV-visible detector set at 216 and 280 nm. Fluorescent compounds were detected with a Perkin-Elmer Life Sciences 650-10S fluorescence spectrophotometer (λ_{ex} = 280 nm, λ_{em} = 410 nm) coupled in-line with the HPLC system. Peak quantification was based on peak area relative to peaks of a chromatogram of authentic standards separated under identical conditions.

RESULTS

Titration of SwMb with H_2O_2—The reaction of SwMb with H_2O_2 produces a peroxidase-like oxoferryl (Fe^{IV}=O) species and a transient protein radical. The relationship between the extent of ferryl formation and the amount of H_2O_2 used in the assay is shown in Fig. 1*A*. Spectra were taken within 6 s following the addition of H_2O_2. The spectrum of SwMb (λ_{max} 504 and 630 nm) changed to that of ferryl Mb (λ_{max} 547 and 575 nm). Comparison of the spectra recorded after each addition of H_2O_2 reveals well defined isosbestic points at 471, 518, 613, and 671 nm, indicating a lack of long-lived intermediates in this conversion process.

Aliquots of the SwMb preparation used in Fig. 1*A* were removed after each addition of H_2O_2, an excess of ascorbate (19 mM) was added to instantly and completely reduce ferryl Mb, and the proportions of the various reaction products were measured by gel filtration chromatography. Typical elution profiles are given in Fig. 1*B*. Intact SwMb appeared as one major peak (*peak 1*). Treatment of the native protein with H_2O_2 led to a decrease in *peak 1* and the appearance of two well defined higher molecular weight peaks, *peak 3* (~52 kDa) and *peak 2* (~38 kDa), that correspond to the SwMb trimer and dimer, respectively.

The ferryl absorbance at 545 nm as a function of the H_2O_2 concentration (*open circles*) is compared with the extent of Mb dimer and trimer formation (*closed circles*) in Fig. 2*A*. The 545-nm curve is composed of two straight line components of differing slopes. Despite a marked curvature, the equivalence points of the titrations can be estimated to within ±10% by measuring the intersection of the extrapolated straight line components of the curve (Fig. 2*A*, *dotted lines*). The intersection occurred at a molar ratio of 1.02 ± 0.08 over three independent determinations. This ratio confirms the 1:1 stoichiometry of metMb and H_2O_2 required for maximal ferryl formation despite several reports to the contrary (see below for plausible explanations for deviation from the exact 1:1 equivalence point of titration). Similarly, the oligomer formation rises to a maximum at a H_2O_2/Mb ratio of 1.4. The maximum yields of the Mb dimer and trimer under these conditions were 28 and 17%, respectively. Above 1.4 eq of H_2O_2, oligomer formation decreases, whereas the ferryl 545-nm absorption continues to rise slowly until 3 eq of H_2O_2 have been added.

The numerical simulations in Fig. 2*B* (*curve 1*) indicate that the curvature of the 545-nm plot can be modeled nicely using the simple model in Scheme 1. *Curve 1* was obtained with the assumption that autoreduction of ferryl Mb to metMb is negligible during the time course of the titration (k_{auto} = 0). Additional simulations (Fig. 2*B*, *curve 2*) indicate that, when the value of k_{auto} in the simulation is set at 2.5×10^{-3} s^{-1} and the other kinetic parameters are maintained constant, the marked curvature and the two straight line segments of the 545-nm curve are still apparent, but the slope of the second part of the

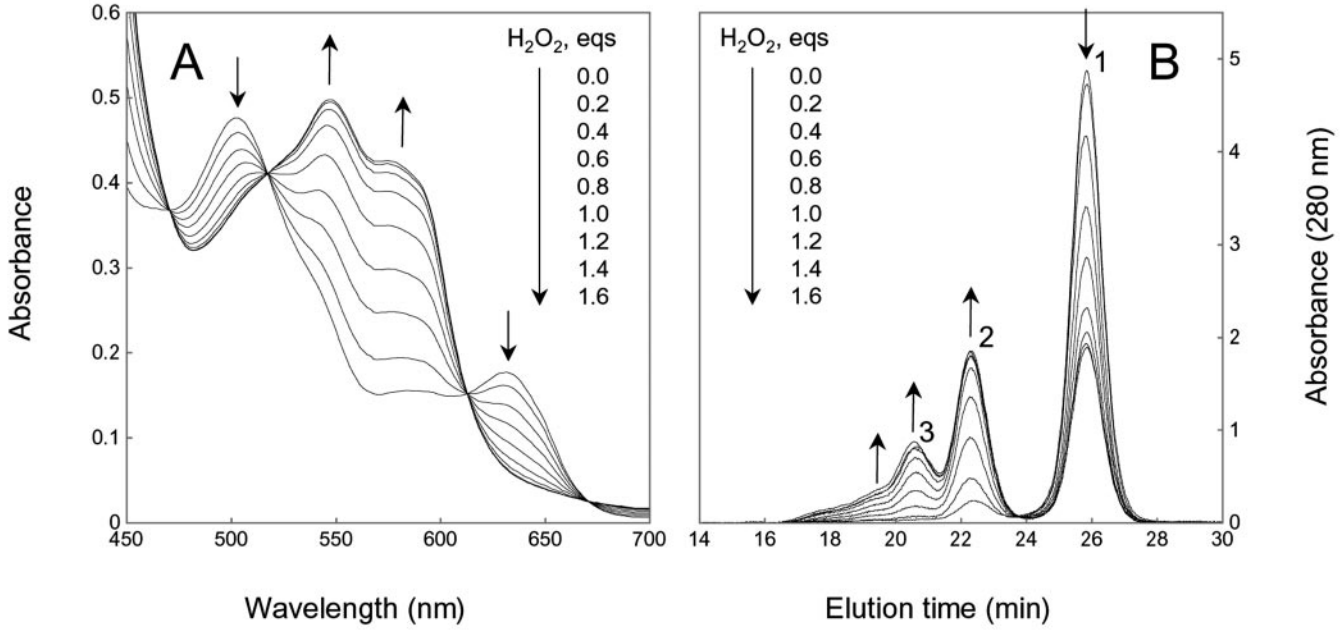

FIG. 1. **Titration of SwMb with H_2O_2.** *A*, spectral changes in the visible region. Experimental conditions were as follows: SwMb (250 μM) in 50 mM potassium phosphate buffer, pH 8.0, at 4 °C. H_2O_2 was added stepwise as indicated, and each spectrum was recorded <6 s after the addition of H_2O_2. The path length of the optical cuvette was 0.2 cm. *B*, variation of elution profiles on a gel filtration column. Aliquots of the reaction mixture were removed after each addition of H_2O_2 and rapidly mixed with ascorbate solutions as described under "Experimental Procedures." The resulting solutions were stored at 4 °C before being chromatographed on a gel filtration column to check the progress of the reaction and the nature of cross-linked products. The directions of spectral and chromatographic changes are indicated by the *arrows*.

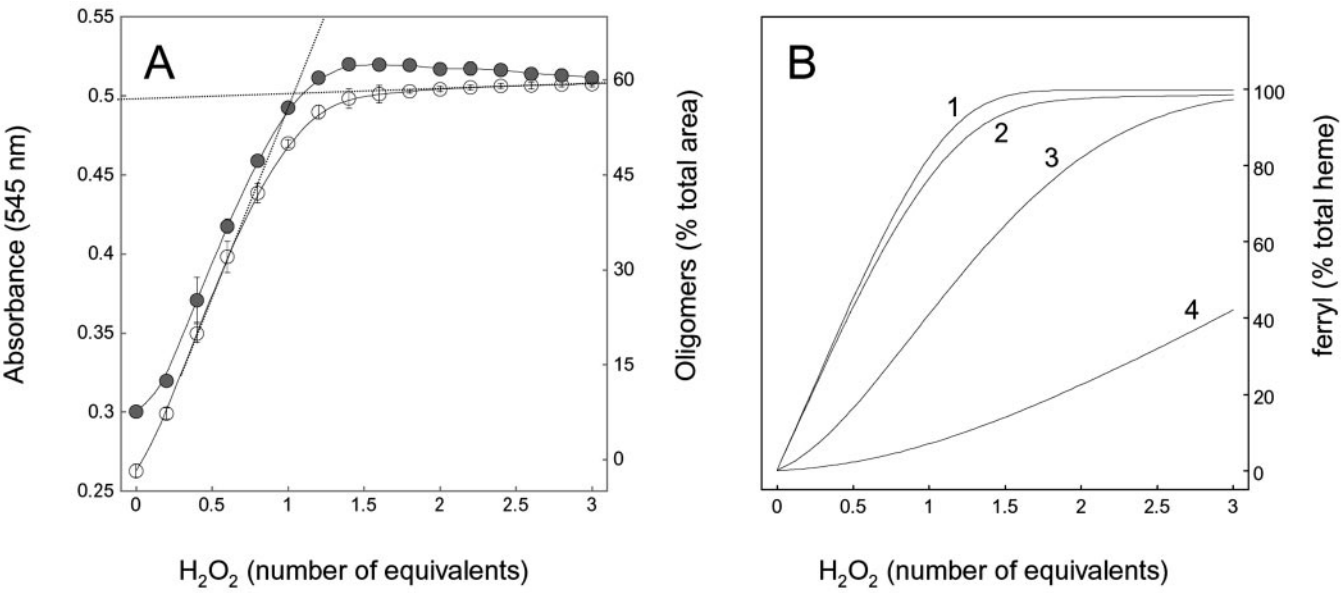

FIG. 2. **Titration of SwMb with H_2O_2.** *A*, correlation of spectral changes at 545 nm (*open circles*) and oligomerization yields (*closed circles*). Experiments were conducted as described in the legend to Fig. 1. The equivalence points were taken as the intersection of extrapolated straight line portions (*dotted lines*). The oligomerization yields were calculated from the gel filtration elution profiles and expressed as a percentage of the chromatographic peak area at 280 nm obtained for metMb before the addition of H_2O_2. Values are mean ± S.D. (n = 3). Where error bars are not visible, they are contained within the *symbol*. *B*, numerical simulations of the variation in the concentration of the ferryl enzyme intermediate as a function of the H_2O_2 concentration. The *curves* are numerical simulations based on the model in Scheme 1. H_2O_2 was added stepwise as indicated in the legend to Fig. 1. The time between two injections was 15 s, and the simulation was done for a 15-s incubation. The kinetic parameters used for *curve 1* were as follows: $k_{12} = 1.8 \times 10^2$ M^{-1} s^{-1}, $k_{13} = 4.9 \times 10^2$ M^{-1} s^{-1}, $k_{23} = 4.0$ s^{-1}, $k_{auto} = 0$. Initial conditions were as follows: [metMb] = 2.5×10^{-4} M, [ferryl Mb] = 0. The kinetic parameters used for *curve 2* were the same as for *curve 1* except $k_{auto} = 2.5 \times 10^{-3}$ s^{-1}. The kinetic parameters used for *curves 3* and *4* were the same as for *curve 1*, except [metMb] = 2.5×10^{-5} M (*curve 3*) or 2.5×10^{-6} M (*curve 4*).

curve, beyond the equivalence point, is now greater than zero. According to these simulations, about 36% of the ferryl Mb molecules in the system are autoreduced to metMb within the time necessary to complete the titration (not shown in the figure). *Curve 1* has been calculated for an initial metMb concentration of 250 μM. *Curves 3* and *4* are the same quantities but calculated for much lower initial metMb concentrations. Under these conditions, the titration curves lack the linear portions needed for end point extrapolation. These results demonstrate that in order to observe a satisfactory photometric end point close to the exact 1:1 equivalence point of titration, it is necessary to use relatively large metMb concentrations. Overall, the numerical simulations indicate that the curvature of the experimental line in Fig. 2*A* results from incomplete for-

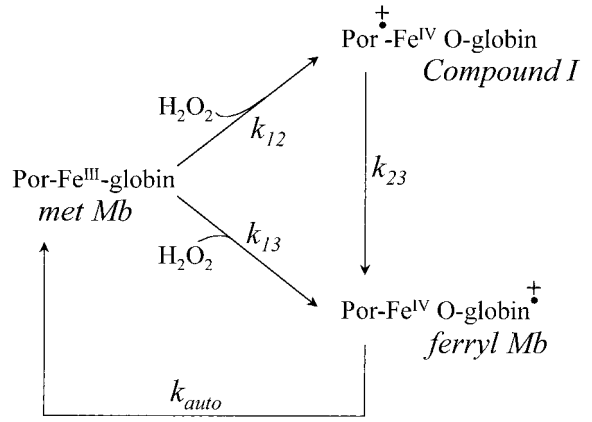

SCHEME 1. **Postulated kinetic scheme for reaction of metmyoglobin with H_2O_2 based on that of Egawa *et al.* (28).** Native metMb can form both Compound I and ferryl Mb upon reaction with H_2O_2. The former is an oxidized intermediate comprising an oxyferryl center, $Fe^{IV}O$, and a porphyrin π-cation radical structure, $Por^{\bullet+}$. The oxidizing equivalent on the porphyrin π-cation is then transferred to the globin moiety of Mb to produce ferryl Mb. Ferryl Mb is reconverted to the resting metMb form by a direct one-step autoreduction reaction. k_{12} and k_{13} are both pseudo-first-order rate constants with respect to H_2O_2 for the formation of Compound I and ferryl Mb from metMb, and k_{23} is the first-order rate constant for the conversion from Compound I to ferryl Mb. k_{auto} is the rate constant for the autoreduction reaction.

mation of ferryl Mb. The non-zero slope of the second part of the curve simply reflects the fact that an appreciable amount of ferryl Mb reverts to metMb during the time course of the reaction.

Dependence of the Oligomerization Yields on the [Mb]/[H_2O_2] Ratio—When the H_2O_2/Mb ratio is held constant at 1.0, the yield of high molecular weight products increases in direct proportion to the protein concentration (Fig. 3*A*). At the highest concentrations of Mb, a new peak can be seen in the *figure* as a distinct shoulder on the edge of *peak 3*. This new peak (*peak 4*) corresponds to tetrameric SwMb with a molecular mass of about 72 kDa. Interestingly, all of the intensity lost from the monomer (*peak 1*) and dimer (*peak 2*) peaks appears as higher molecular weight products (*peaks 3* and *4*). Furthermore, oligomer formation increases to a maximum as the H_2O_2/Mb ratio rises to a value between 1 and 2 (Fig. 3*B*). Above 2 eq there is a progressive decrease in oligomer accumulation. The decrease is small but was seen consistently with various SwMb preparations. Regardless of the H_2O_2/Mb ratio and the protein concentration, the monomer was never completely consumed.

The amounts (Table I) of the cross-linked products formed with the H_2O_2/Mb ratio set at 1.0 were quantitated by deconvolution of the chromatographs in Fig. 3*A*. Di-, tri-, and tetrameric products were predominantly formed in the range of protein concentrations investigated. As the oligomerization of SwMb is due to dityrosine and isodityrosine cross-links formed by the coupling of two tyrosine radicals, radicals must be present on both tyrosine residues for efficient coupling. It is therefore possible to calculate the number of oxidation equivalents utilized in the formation of the different cross-linked products from their absolute concentrations (last column in Table I). The data indicate that (*a*) SwMb oligomerization consumes a major fraction of the oxidizing equivalents in the system, and (*b*) as the concentration of SwMb increases, oligomerization consumes an increasing fraction of the available oxidizing equivalents.

Characterization of Monomeric and Dimeric Forms of H_2O_2-treated SwMb—Upon incubation with H_2O_2, the monomeric protein was partially converted to oligomeric products (Figs. 1*B* and 2). Additional experiments were conducted to characterize both the remaining monomeric protein and the dimeric product. The two products were purified to homogeneity by repeated passage through a gel filtration column as detailed under "Experimental Procedures." The UV-visible spectra of the purified products after autoreduction to the ferric form were very similar in the Soret (350–450 nm) and visible (450–700 nm) regions of the spectrum to that of the native enzyme (not shown), indicating that the heme environment of the enzyme was minimally altered. Each of the purified products reacted with H_2O_2 to form a species with a spectrum essentially identical to that of the ferryl Mb formed from the native enzyme (not shown). To estimate the degree of alteration of the prosthetic heme group, the monomeric and dimeric forms of H_2O_2-treated SwMb were injected onto an HPLC column under conditions that separate noncovalently bound porphyrins from those covalently attached to the protein. Quantitation of the heme species (Table II) indicates that only a small fraction of the heme (less than 2%) was either covalently bound or oxidatively modified. In contrast, only unmodified heme was found in native SwMb. This was not unexpected, since the treatment of metMb with H_2O_2 was done at pH 6.8, at which alteration of the prosthetic heme group and formation of protein-bound products are minimal. Fig. 4 shows the profile of the purified products on a gel filtration column. The elution profiles before and after incubation with H_2O_2 are given in the same *figure* for comparison. The molecular weights of the proteins after incubation with H_2O_2 were also determined on an SDS-polyacrylamide gel (Fig. 4, *inset*). When the recovered monomeric protein was again exposed to H_2O_2, two new peaks (*peaks 2* and *3*, Fig. 4*A*) occurred at positions corresponding to M_r ~38,000 and ~52,000, in agreement with the formation of dimeric and trimeric products. Within experimental error, the yield of oligomeric products obtained from the recovered monomer upon reaction with H_2O_2 was similar to that from native SwMb (not shown). Under similar experimental conditions, treatment of the dimer with H_2O_2 led to a decrease of *peak 2* (Fig. 4*B*) and the appearance of both low and high molecular weight peaks (*peaks 1* and *3*, respectively (Fig. 4*B*)). SDS-PAGE analysis showed that *peak 2* corresponded to a dimeric product, and *peak 3* is consistent with the formation of both trimeric and tetrameric products. *Peak 1* migrates in the same position as the monomer. This band was consistently more abundant in the H_2O_2-treated samples of the dimer (compare the trace before and after the addition of H_2O_2), which suggests that a fraction of the dimer is oxidatively cleaved during incubation with H_2O_2.

Separation and Identification of Tyrosine-derived Radical Addition Products—We showed some time ago that a fraction of the tyrosine residues lost during the dimerization of SwMb is converted to unidentified products other than dityrosine (15). This led us to investigate whether other tyrosyl radical products are generated during the oligomerization of SwMb. SwMb was mixed with 1.0 eq of H_2O_2, and, after a short incubation, the monomeric and dimeric oxidation products were separated and purified to homogeneity by repeated passage through a gel filtration column. The oxidation products were then sequentially digested with an endopeptidase, a carboxypeptidase, and an aminopeptidase. Separation of the proteolytic digest by HPLC revealed a number of peaks detected by fluorescence at 410 nm (Fig. 5, *A* and *B*) or by absorbance at 280 nm (Fig. 5, *D* and *E*). Preliminary peak identification was based on comparison of retention times with authentic standards separated under identical conditions. There are three Tyr and two Trp residues in SwMb, and the chromatograms of proteolytic digests of the native protein exhibited the expected peaks of Tyr and Trp at 13.4 and 33.4 min, respectively. In the case of the

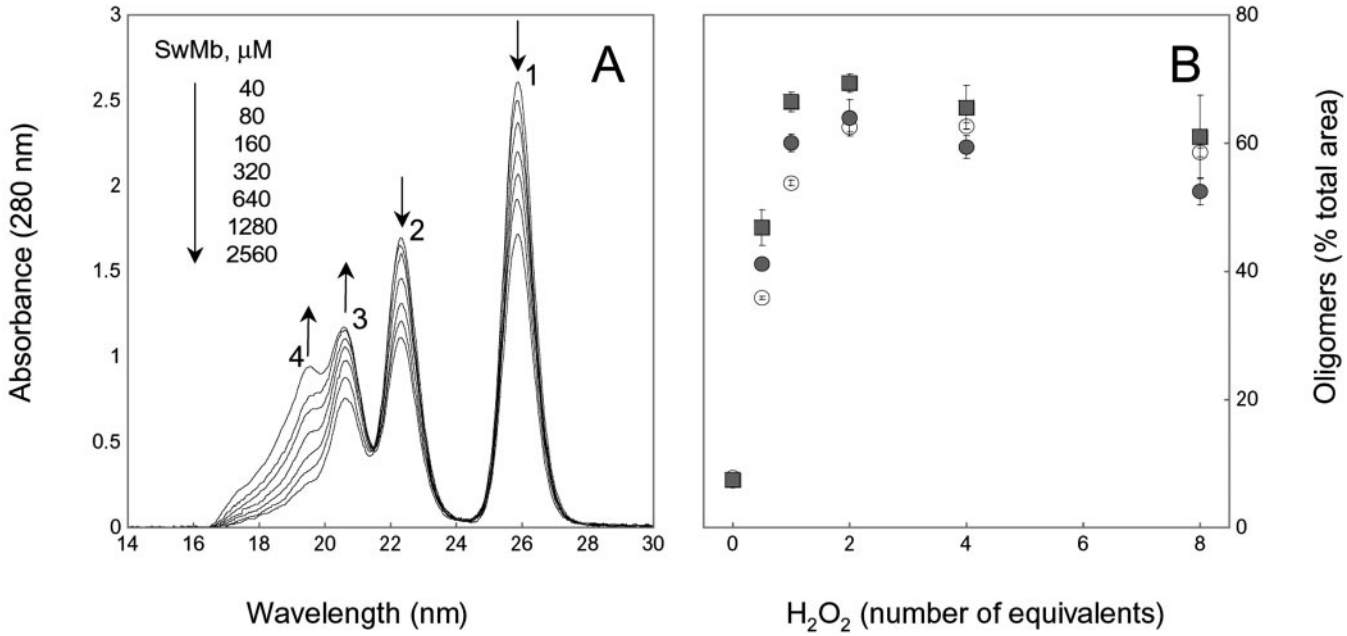

FIG. 3. **Dependence of the oligomerization reaction on the Mb concentrations and on [Mb]/[H_2O_2] ratios.** *A*, effect of increasing Mb the concentration on elution profiles. Experimental conditions were as follows: SwMb (40–2560 μM) in 50 mM potassium phosphate buffer, pH 6.8, at 25 °C. The reaction was initiated by the addition of 1 eq of H_2O_2. The resulting solutions were stored at 4 °C for 24 h before being chromatographed on a gel filtration column. The directions of chromatographic changes are indicated by the *arrows*. *B*, dependence of the oligomerization yields on H_2O_2 concentration for three different Mb concentrations: 40 μM SwMb (○), 250 μM SwMb (●), and 1500 μM SwMb (□) in 50 mM potassium phosphate buffer, pH 6.8, at 25 °C. The reaction was initiated by the addition of stock solutions of H_2O_2 to give the desired H_2O_2/SwMb ratio. The oligomerization yields were calculated and expressed as described under "Experimental Procedures." Values are mean ± S.D. (n = 3).

TABLE I

Relative amount of cross-linked products formed and of oxidation equivalents utilized in forming cross-linked products after treatment of SwMb with a stoichiometric amount of H_2O_2

SwMb concentration	Percentage of total Mb chain[a]				Equivalents utilized[b]
	Dimer	Trimer	Tetramer	Oligomer	
μM	%	%	%	%	%
40	32.5 ± 0.2	11 ± 4	7 ± 6	1 ± 3	30 ± 6
80	31.4 ± 0.2	14 ± 3	8 ± 6	2 ± 4	32 ± 6
160	29.4 ± 0.2	15 ± 3	10 ± 6	3 ± 3	35 ± 5
320	27.8 ± 0.2	17 ± 2	11 ± 4	5 ± 3	37 ± 4
640	25.2 ± 0.2	18 ± 2	15 ± 2	5.1 ± 0.9	39 ± 2
1280	23.7 ± 0.2	18 ± 2	14 ± 5	10 ± 4	42 ± 5
2560	21.6 ± 0.2	16 ± 1	22 ± 4	9 ± 3	46 ± 3

[a] The relative amounts of cross-linked products formed were calculated by deconvolution of the FPLC traces in Fig. 3*A* as described under "Experimental Procedures." The number of Gaussian peaks contained in each chromatograph was fixed to 5.

[b] The formation of dimeric, trimeric, tetrameric, and oligomeric products was assumed to require 1.00, 1.33, 1.50, and 1.60 eq per Mb chain, respectively. A yield of 100% is expected if all of the oxidation equivalents present in the incubation (e.g. 2 eq per Mb chain) are quantitatively utilized in forming cross-linked products.

TABLE II

Heme species in monomeric and dimeric forms of H_2O_2-treated SwMb as compared with the native form

Samples were purified to homogeneity by repeated passage through a gel filtration column and were analyzed by HPLC, as described under "Experimental Procedures."

	Percentage of total heme[a]		
	Unmodified heme	Covalently bound heme	Oxidatively modified polar heme
	%	%	%
Monomer native form	100 ± 3	ND[b]	ND[b]
H_2O_2-treated dimer	98 ± 3	1.4 ± 0.1	0.547 ± 0.002
H_2O_2-treated monomer	99 ± 5	0.6 ± 0.4	0.700 ± 0.045

[a] The relative amounts of the different heme species formed were quantified from the HPLC peak areas at 400 nm. Values are mean ± S.D. (n = 3).

[b] ND, not detectable.

dimer, fluorescence detection showed the presence of an additional minor peak that eluted at 20.8 min. The excitation and emission spectra of this product after isolation were virtually identical to those of dityrosine at both acidic and alkaline pH (not shown). The identity of this fluorescent compound with dityrosine was confirmed by co-migration with an authentic sample (Fig. 5*C*). The UV detection of the dimer hydrolysates also revealed a new peak at 26.4 min that co-migrated with isodityrosine (Fig. 5, *E* and *F*). Isodityrosine exhibits 280 nm UV absorbance but no 410-nm fluorescence emission upon excitation at 280 nm. Consistent with these properties, the peak was only observed with UV detection (Fig. 5*E*). This finding excludes the possibility that the product eluting at 26.4 min results from dityrosine-containing peptides, since these peptides would be detected by the fluorescence detector. The product eluting at 26.4 min was isolated and shown by electrospray ionization mass spectrometry in the negative ion mode to have a molecular ion $(M - H)^-$ at m/z 358.8, as expected for a tyrosine dimer. This mass spectrum, together with co-migration on HPLC with an authentic sample, conclusively identifies the adduct as isodityrosine. As a control, protease blanks in which a sample of the protease mixture incubated without metMb was worked up exactly in the same way as the Mb digest showed minor peaks with the retention times of Trp and Tyr (not shown). This indicates that the proteases tend to self-digestion, but the chromatogram of the protease mixture did not contain the dityrosine and isodityrosine peaks.

Content of Tyrosine and Tyrosine-derived Cross-links—The contents of tryptophan, tyrosine, and the two tyrosine-derived cross-links in the monomer and dimer of the native protein purified by gel filtration chromatography were determined by

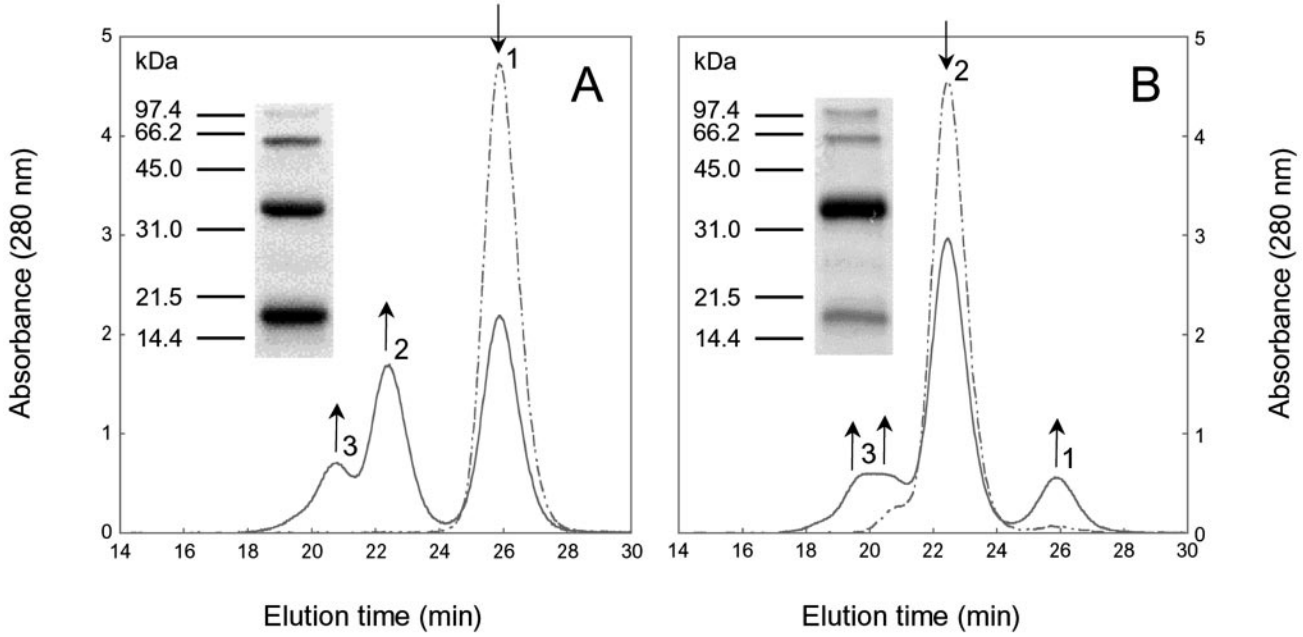

FIG. 4. **Gel filtration chromatography and SDS-PAGE analysis of the monomeric and dimeric products.** *A*, elution profiles of purified the monomeric products before (*broken line*) and after (*solid line*) incubation with 2 eq of H_2O_2. *Inset*, SDS-PAGE analysis ([polyacrylamide] = 20%) of the monomeric products after incubation with 2 eq of H_2O_2. The samples were reduced with 2-mercaptoethanol and were boiled before electrophoresis. *B*, as in *A* but with the dimeric form of SwMb. The following concentrations were used: [Mb] = 40 μM in heme, [H_2O_2] = 80 μM.

proteolysis and HPLC (Table III). The tryptophan and tyrosine contents of native SwMb were in agreement with the known composition of the protein. Incubation with H_2O_2 had no effect on the tryptophan content but decreased the tyrosine content of the dimer by 47% and of the recovered monomer by 14%. No tyrosine-derived cross-links could be detected in native SwMb or the recovered monomer, but isodityrosine and dityrosine were found in the SwMb dimer hydrolysates at levels of 15.2 and 6.8% of the theoretical yield, respectively. The remaining 25% of the tyrosine lost in the dimers cannot be accounted for by the formation of dityrosine or isodityrosine cross-links. Control experiments with authentic tryptophan, tyrosine, dityrosine, and isodityrosine showed that the hydrolysis conditions cause no more than small changes (<3.5%) in the concentrations of these residues. Some tyrosine loss thus occurs by reactions other than tyrosine-tyrosine formation during the reaction of SwMb with H_2O_2.

Involvement of Specific Tyrosine Residues—There are three tyrosine residues in SwMb (Tyr^{103}, Tyr^{146}, and Tyr^{151}). To identify the site of cross-linking, the triple mutant K102Q/Y103F/Y146F was expressed, and its susceptibility to form dityrosine and isodityrosine cross-links was examined. The Lys → Gln substitution at position 102 stabilizes proteins with the Tyr^{103} mutation (17). Incubation of the SwMb triple mutant with H_2O_2 resulted in the formation of monomeric and dimeric products (not shown). The monomeric and dimeric forms were separated by gel filtration FPLC. Proteolytic digestion of the gel-purified forms was carried out, and the digests were analyzed by HPLC. Table IV lists the contents of tryptophan, tyrosine, and the two tyrosine-derived cross-links in the monomeric and the dimeric mutant proteins. The tryptophan and tyrosine contents of the native protein were in agreement with the known composition of the mutant. No tyrosine-derived cross-links could be detected in the native form of the mutant or the recovered monomer. Both isodityrosine and dityrosine could be detected in protein hydrolysates of the dimeric mutant protein. Interestingly, the area of the isodityrosine peak was similar to that seen for the native dimeric protein. The results unambiguously established that isodityrosine links between the myoglobin chains are primarily forged by coupling of Tyr^{151} of one chain with Tyr^{151} of the other.

The stoichiometry of the reaction of SwMb with H_2O_2 suggests that the monomer undergoes a two-electron oxidation. One of the two oxidation equivalents is accounted for by oxidation of Fe(III) to the Fe(IV) ferryl species, and the second oxidation equivalent is rapidly dissipated into protein-centered radicals, some of which couple to yield dimeric products. Formation of trimeric and higher oligomeric entities linked by dityrosine bonds requires that a second oxidation equivalent be located, at least transitorily, on the protein surface. This second protein radical must be produced by an inter- or intraradical transfer among the proteins present in the incubation.

Intermolecular Radical Transfer Reaction—The possibility of intermolecular radical transfers in the SwMb/H_2O_2 system was investigated by removing the prosthetic group from SwMb. This precludes direct activation of the SwMb by H_2O_2. The apoMb thus obtained was then incubated with the heme-containing Y151F SwMb mutant and H_2O_2, and the incubation mixture was analyzed for the formation of cross-linked products (Fig. 6). SwMb has three tyrosines, Tyr^{103}, Tyr^{146}, and Tyr^{151}, but site-directed mutagenesis studies have shown that only Tyr^{151} is absolutely critical for protein oligomerization (17). Thus, the Y151F mutant can react with H_2O_2 but cannot itself dimerize. Oligomer formation is therefore only possible if the radical generated by reaction of the Y151F mutant with H_2O_2 is transferred to the apoSwMb. When the apoSwMb/holo-Y151F SwMb mixture was exposed to H_2O_2, two new products of M_r 36,000 and 44,000, corresponding to the dimer and trimer, were formed (Fig. 6, *lane 5*). Control experiments confirm that neither the apoMb nor the holo form of the Y151F mutant dimerizes to an appreciable extent (*lanes 2* and *4*, respectively). Significant oligomerization only occurred when the apoSwMb/holo-Y151F SwMb mixture was exposed to H_2O_2. Thus, the oligomerization observed in this experimental protocol establishes that a radical was transferred from the Y151F SwMb mutant to the apoSwMb.

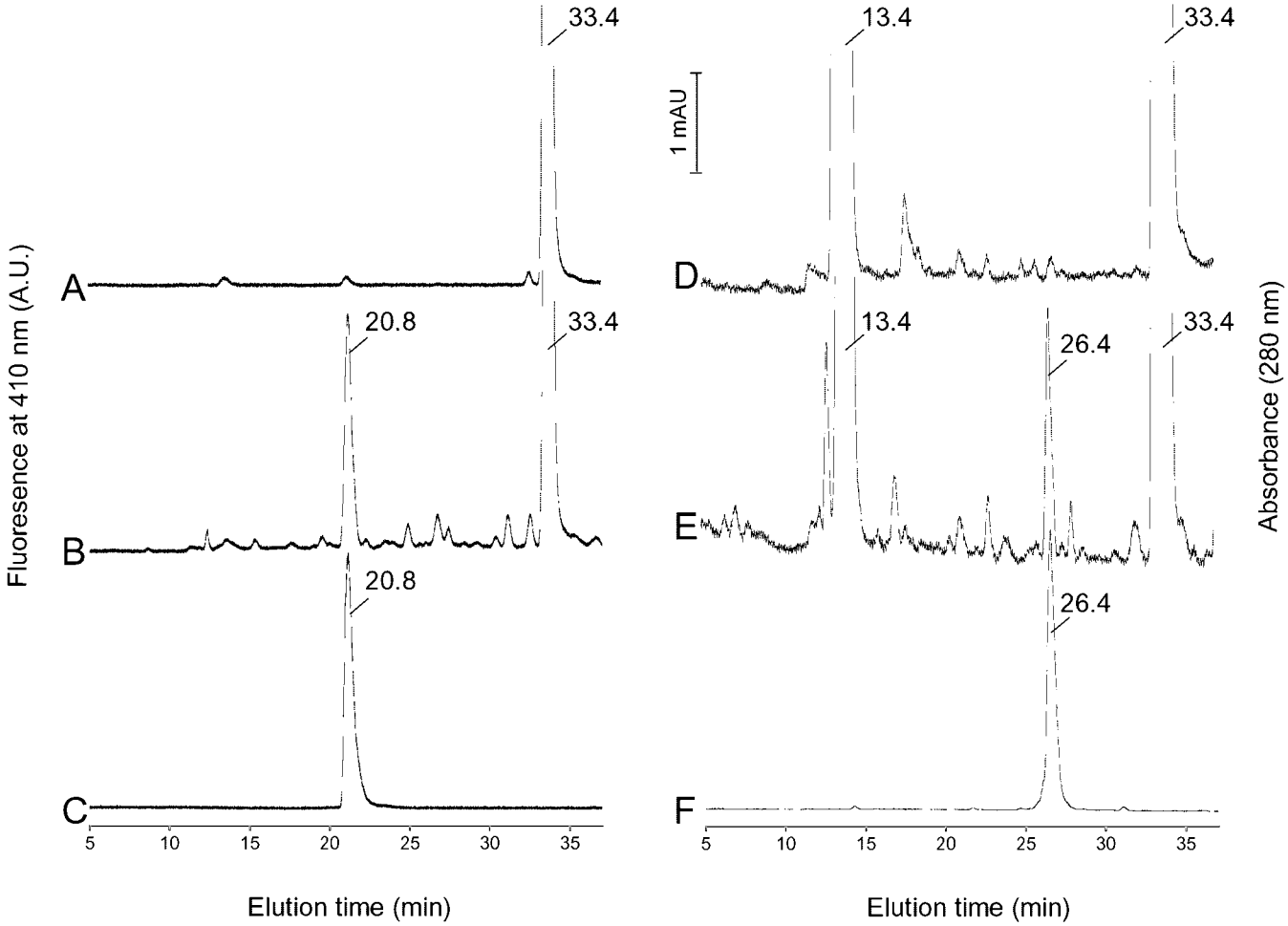

FIG. 5. **Reverse phase HPLC analysis of Mb hydrolysates and of a dityrosine standard.** *A* and *D*, native SwMb; *B* and *E*, dimeric form of H_2O_2-treated SwMb; *C*, dityrosine standard; *F*, isodityrosine standard. *Curves A*, *B*, and *C*, fluorescence intensity changes monitored at 410 nm (excitation 280 nm); *curves D*, *E*, and *F*, absorption changes monitored at 280 nm.

TABLE III
Contents of tryptophan, tyrosine, and tyrosine-derived cross-links of wild-type SwMb
The hydrolysis and analytical conditions are described under "Experimental Procedures." Values are mean ± S.D. (n = 3). ND, not detectable.

	Amino acid residues/Mb chain			
	Tryptophan	Tyrosine	Dityrosine	Isodityrosine
Monomer native form	2.01 ± 0.08	2.96 ± 0.18	ND	ND
H_2O_2-treated dimer	2.08 ± 0.06	1.57 ± 0.10	0.034 ± 0.002[a] (6.8%)[b]	0.076 ± 0.008[a] (15.2%)[b]
H_2O_2-treated monomer	2.05 ± 0.01	2.55 ± 0.04	ND	ND

[a] A cross-link content of 0.5 amino acid/Mb chain is expected if one tyrosine of each Mb chain is quantitatively converted to a dityrosine or a isodityrosine cross-link.
[b] The relative yields (in parentheses) are given as percentages of the theoretical yield, which is one cross-link per two Mb chains.

Intramolecular Versus Intermolecular Radical Transfer Reaction: Autoreduction of Ferryl Mb to MetMb—Fig. 7*A* shows the visible absorption changes during the autoreduction of ferryl Mb to metMb. Native metMb was converted into ferryl Mb by the addition of 2.4 equivalents of H_2O_2. After 10 s, the excess of H_2O_2 was removed by adding catalase. The spectrum at 0 min (λ_{max} 547 and 575 nm) is that of the resulting ferryl Mb. On standing, the ferryl Mb was slowly converted back to metMb (λ_{max} 504 and 630 nm). The absence of well defined isosbestic points suggests a complex reversion pattern. Furthermore, the product of the decay has a spectrum, as shown by the *dotted line* in Fig. 7*A*, that differs slightly from that of the native protein.

The time course of the autoreduction followed at 545 nm, the absorption maximum of the ferryl form, is complex, and at least two exponentials are required to adequately fit the absorbance changes (Fig. 7*B*, *lower panel*). The fast phase is well separated from the slow phase, and the rate constant and the amplitude for the two phases of the reaction could be determined accurately. The fast exponential phase of the reduction is complete within minutes (*curve 2*, t = 3.4 min), whereas the subsequent slow phase occurs on a time scale of minutes to hours (*curve 3*, t_2 = 25.9 min). The amplitude of the fast phase corresponds to reduction of 42% of the ferryl species. The effect of the initial ferryl Mb concentration on ferryl autoreduction shows that at [SwMb] ≤ 40 μM, the $k_{1\ obs}$ and $k_{2\ obs}$ values and the amplitude for the two phases of the reaction were independent of the initial ferryl concentration (Table V). This finding indicates that Fe^{IV}=O reduction occurs via an intramolecular electron transfer. At higher protein concentrations, the amplitude of the fast phase increased as the protein concentration increased. The results in Table I show that oligomerization is enhanced by

TABLE IV
Contents of tryptophan, tyrosine, and tyrosine-derived cross-links of K102Q/Y103F/Y146F site-directed mutant

A limited amount of the K102Q/Y103F/Y146F mutant was available because of low expression yields of this mutant. Values are for one experiment. The hydrolysis and analytical conditions are described under "Experimental Procedures." ND, not detectable.

	Amino acid residues/Mb chain			
	Tryptophan	Tyrosine	Dityrosine	Isodityrosine
Monomer native form	2.05	1.11	ND	ND
H_2O_2-treated dimer[a]	1.91	0.41	0.012[b] (2.4%)[c]	0.059[b] (11.8%)[c]
H_2O_2-treated monomer	1.99	0.95	ND	ND

[a] This preparation was only partially purified because of the limited amount of material available. Deconvolution of the FPLC traces showed that the preparation contains about 30% of monomer.
[b] A cross-link content of 0.5 amino acid/Mb chain is expected if one tyrosine of each Mb chain is quantitatively converted to a dityrosine or a isodityrosine cross-link.
[c] The relative yields (in parentheses) are given as percentages of the theoretical yield, which is one cross-link per two Mb chains.

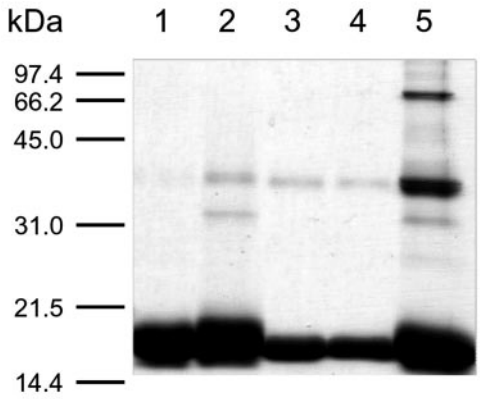

FIG. 6. **SDS-PAGE analysis of the cross-linking between ApoSwMb and the Y151F mutant.** *Lane 1*, apoMb; *lane 2*, apoMb + H_2O_2; *lane 3*, Y151F mutant; *lane 4*, Y151F mutant + H_2O_2; *lane 5*; apoMb + Y151F mutant + H_2O_2. The following concentrations were used: [apoMb] = 40 μM; [Y151F mutant] = 100 μM; [H_2O_2] = 100 μM; [polyacrylamide] = 16%. The samples were reduced with 2-mercaptoethanol and were boiled before electrophoresis.

high protein concentrations. To determine whether oligomerization reduces the lifetime of the ferryl species, the experiments were repeated with the monomeric and oligomeric fractions of SwMb isolated by FPLC gel filtration and, for control purposes, with the native form of the enzyme. The results in Table VI indicate that oligomerization had no significant effect on the $k_{1\,obs}$ and $k_{2\,obs}$ values of the reaction. However, the amplitudes for the fast phase of the reaction obtained with the oligomeric products were substantially larger than those obtained with the native protein. The kinetic parameters obtained with the remaining monomeric protein, on the other hand, did not differ significantly from those obtained with the native protein. The above results strongly suggest that the oligomerization decreases the lifetime of the ferryl species.

Formation of Oligomeric Products during the Autoreduction Phase—The influence of SwMb concentration on the amount of cross-linked products formed during the conversion of the ferryl form back to the ferric resting state is presented in Table VII. Native metMb was converted into ferryl Mb by the addition of a large excess of H_2O_2. After 10 s, the excess of H_2O_2 was removed by adding catalase, and aliquots of the preparation were taken at the time indicated and rapidly quenched with ascorbate. The resulting mixtures were analyzed by gel filtration FPLC to determine the yields of oligomeric products. In all experiments, more than 70% of the oligomerization occurs during the initial mixing time of the experiments. The result indicates that the major fraction of the oligomeric products is formed immediately after myoglobin activation (*e.g.* before the autoreduction phase). When the reaction was carried out with 10 μM SwMb, the amount of oligomers formed was independent of the time of stopping the reaction. Waiting 10 h gave similar results (no significant differences) as analysis 1 min after myoglobin activation by H_2O_2. The absence of a time dependence suggests that the cross-links are formed immediately after the activation of myoglobin and the oligomerization ceases when the heme is in the ferryl form. At higher protein concentrations, a small but significant fraction of the oligomers was formed between 5 min and 10 h after myoglobin activation. This latter result suggests that, under these conditions, protein-centered radicals generated during autoreduction of the ferryl species also lead to the formation of oligomeric products.

Autoreduction of Oligomerization-resistant Monomer—As shown above, native monomeric protein was only partially converted to oligomeric products, whatever the protein and H_2O_2 concentration (Figs. 1*B* and 2). To determine the basis for this resistance to oligomerization, the remaining monomeric protein was separated from the higher molecular products by gel filtration chromatography, and the absorption spectrum of the recovered monomer was recorded at various time points to quantitate the extent to which it was present in the ferryl form. After suitable dilution, the samples were also rapidly mixed with excess H_2O_2, and the resulting solutions were analyzed by FPLC to estimate the yields of cross-linked proteins.

The time course for autoreduction of the recovered monomer (*open circles*) and its capacity to oligomerize when reexposed to H_2O_2 (*open triangles*) are shown in Fig. 8*A*. The first measurements were carried out 30 min after the addition of H_2O_2 (*e.g.* a few minutes after elution of the monomer peak from the FPLC column). The results indicate that reaction with H_2O_2 increases the amount of the protein in the ferryl form and alters the extent of oligomerization. Thus, the oligomerization yield of the starting preparation with 43% of the heme in the ferryl form was 46% lower upon treatment with H_2O_2 than that obtained with native SwMb (Fig. 8*A*). Moreover, similar measurements obtained after the ferryl moiety was allowed to decay for a further 2 h indicate that the inhibition of oligomerization is reversible (Fig. 8*A*). A plot of the percentage of inhibition of oligomerization *versus* the fraction of the protein in the ferryl form, determined from the *curves* in Fig. 8*A*, shows that inhibition approaches 100% as the fraction of the protein in the ferryl form approaches 100% (Fig. 8*B*). Oligomerization thus ceases when the heme is in the ferryl form and resumes when the ferryl form reverts to the ferric form.

DISCUSSION

The formation of protein-centered radicals in the reactions of SwMb with H_2O_2 was first reported in 1958 and since then has been amply confirmed (*e.g.* see Refs. 12–14). Nevertheless, the precise location of the radical in the protein and the detailed mechanism by which it is formed remain unclear. Good evidence exists for the formation of Tyr^{103} and Tyr^{151} tyrosyl radicals in SwMb (15, 17, 18, 45), the location of unpaired electron density on Trp^{14} (18, 24), and the possible presence of additional radical sites, notably at Lys^{42} in SwMb and Cys^{110} in human Mb (25, 26). Tyr^{103} is immediately adjacent to the heme group and is thus optimally placed for oxidation by the ferryl species. Tyr^{151} and Trp^{14}, however, are located at some distance from the heme edge. The mechanisms that allow translocation of the unpaired electron from one site to another, whether different radical centers are formed in parallel sequentially, and whether they are in equilibrium or are irrevers-

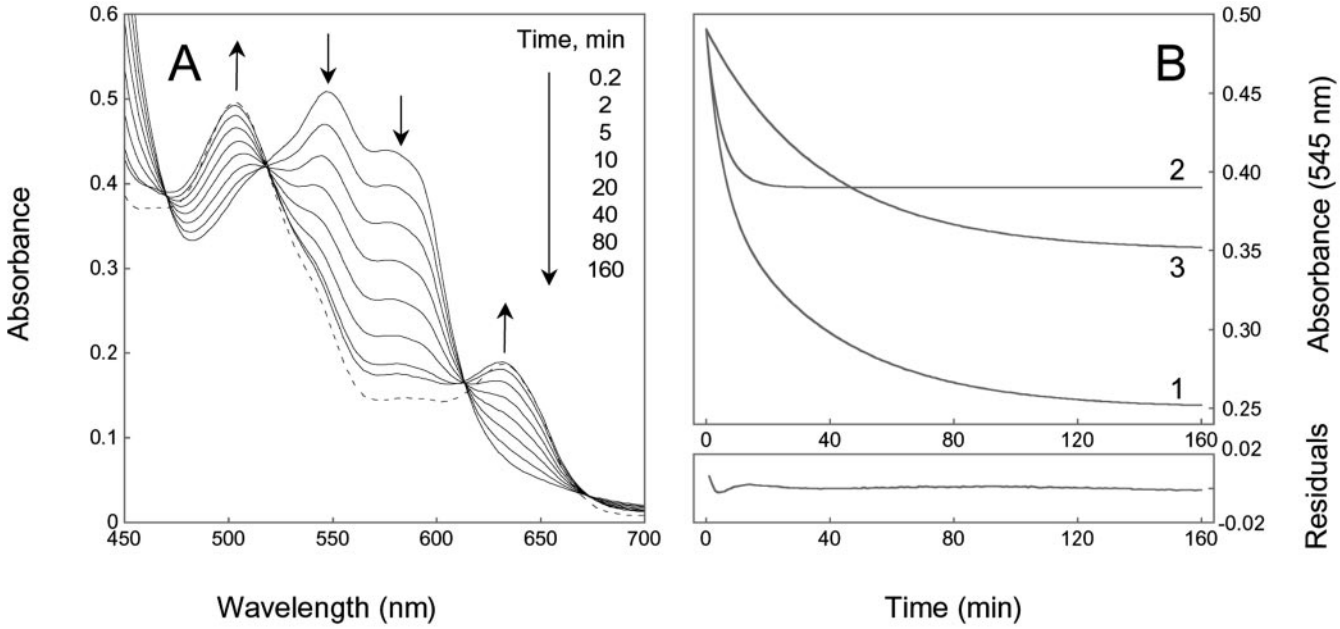

FIG. 7. **Autoreduction of ferryl Mb to metMb.** *A*, spectral changes in the visible region. Experimental conditions were as follows: SwMb (250 μM) in 50 mM potassium phosphate buffer, pH 6.8, at 25 °C. The reaction was initiated by the addition of H_2O_2 at a final concentration of 600 μM. After a 10-s incubation, the excess of H_2O_2 was removed upon the addition of catalase (26 units), and scans were taken at the time intervals indicated. The *broken line* in *A* is the spectrum obtained for metMb before the addition of H_2O_2, and other scans were recorded after the initiation of the reaction. The path length of the optical cuvette was 0.2 cm. *B*, time course of the autoreduction reaction at 545 nm (absorption maximum of the ferryl form). *Curve 1* shows a fit of $A(t) = a + b \exp(-k_{1\ obs}\ t) + c \exp(-k_{2\ obs}\ t)$ to the experimental points. *Curves 2* and *3* represent, respectively, the fast and the slow phases of exponential decay. The parameters (amplitudes and exponential coefficients) for the *curves* are those calculated by the method described under "Experimental Procedures." The *lower panel* shows residuals from a nonlinear regression analysis: $A(t) = a + b \exp(-k_{1\ obs}\ t) + c \exp(-k_{2\ obs}\ t)$, from which $k_{1\ obs} = 0.203\ min^{-1}$ and $b = 0.100$ for the fast phase, and $k_{2\ obs} = 0.027\ min^{-1}$ and $c = 0.140$ for the slow phase, are obtained.

TABLE V
Concentration dependence of the kinetic parameters for the autoreduction of ferryl Mb to metMb

Assay conditions were as follows: SwMb (5–640 μM) in 50 mM potassium phosphate buffer, pH 6.8, at 25 °C. The reaction was initiated by the addition of H_2O_2 at a final concentration of 640 μM. After a 10-s incubation, the excess H_2O_2 was removed upon the addition of catalase (26 units). The kinetic parameters for each Mb concentration were estimated from fits of $A(t) = a + b \exp(-k_{1\ obs}\ t) + c \exp(-k_{2\ obs}\ t)$ to absorbance changes at 421 and/or 545 nm (absorption maxima of the ferryl form).

SwMb concentration	Fast phase		Slow phase	
	b	$k_{1\ obs} \times 10^3$	c	$k_{2\ obs} \times 10^4$
μM	%	s^{-1}	%	s^{-1}
5	29 ± 6	3.5 ± 0.9	71 ± 6	3.4 ± 0.5
10	29 ± 6	3.8 ± 0.2	71 ± 6	3.3 ± 0.3
40	31 ± 5	3.0 ± 0.6	69 ± 5	3.9 ± 0.1
160	37 ± 1	3.2 ± 0.7	63 ± 1	3.8 ± 0.3
640	45 ± 1	4.1 ± 0.5	55 ± 1	5.2 ± 0.3

TABLE VI
Kinetic parameters for the autoreduction of ferryl Mb to metMb of the main protein fractions isolated on the gel filtration column as compared with native form

Assay conditions were as follows: SwMb (5 μM) in 50 mM potassium phosphate buffer, pH 6.8, at 25°C. The reaction was initiated by the addition of H_2O_2 at a final concentration of 400 μM. A large excess of H_2O_2 was used in all experiments to ensure complete conversion of the metMb to the ferryl form within 10 s. After a 10-s incubation, the excess H_2O_2 was removed upon the addition of catalase (26 units). The kinetic parameters for each Mb concentration were estimated from fits of $A(t) = a + b \exp(-k_{1\ obs}\ t) + c \exp(-k_{2\ obs}\ t)$ to absorbance changes at 421 nm (absorption maximum of the ferryl form).

	Fast phase		Slow phase	
	b	$k_{1\ obs} \times 10^3$	c	$k_{2\ obs} \times 10^4$
	%	s^{-1}	%	s^{-1}
Native form	29 ± 6	3.5 ± 0.9	71 ± 6	3.4 ± 0.5
Monomeric product	31 ± 1	3.8 ± 0.2	69 ± 1	3.31 ± 0.06
Dimeric product	45 ± 1	3.5 ± 0.2	55 ± 1	3.6 ± 0.2
Trimeric product	52 ± 1	3.48 ± 0.04	48 ± 1	4.05 ± 0.06

ibly generated, remain open questions. Although formulated in the context of SwMb, these are general questions that apply to many protein radical systems. The reaction of Mb with H_2O_2 has proven to be a very useful prototypical system for the examination of such questions because (*a*) Mb is small and robust, (*b*) the Mb structure has been extensively characterized and is known at high resolution, (*c*) Mb has a limited number of highly oxidizable residues (two tryptophans and up to three tyrosines), and, most importantly, (*d*) the site to which the protein electron is transferred, the heme, can be specified, and its location can be precisely defined.

As part of a continuing effort to address such questions, we have investigated the relationship between the reaction of SwMb with H_2O_2 and the formation of oligomeric products. Previous studies have shown that this reaction yields SwMb dimers linked by a dityrosine bond between Tyr^{151} of one monomer and Tyr^{103} of the other (15). Furthermore, mutagenesis of Tyr^{103} and/or Tyr^{146} to a Phe does not interfere with dimer formation, whereas analogous mutation of Tyr^{151} completely blocks dimerization (17, 18). This implies that Tyr^{151}-Tyr^{151} cross-links are present in the dimer population in addition to the previously identified Tyr^{151}-Tyr^{103} cross-links. The present studies show that SwMb gives not only the previously reported dimers but also a residual, dimerization-resistant monomer as well as trimeric and even tetrameric products. To more precisely characterize the cross-links in these proteins, we have isolated the dimer and oligomerization-resistant monomer. The observation that the UV-visible spectra of the dimer and recovered monomer after autoreduction to the ferric form following the first round of oligomerization are indistinguishable from those of native SwMb indicates that the reaction with H_2O_2

TABLE VII
Relative amount of cross-linked products formed during the conversion of the ferryl form back to the ferric resting state

Assay conditions were as follows: SwMb (10–2560 μM) in 50 mM potassium phosphate buffer, pH 6.8, at 25°C. The reaction was initiated by the addition of H_2O_2 at a final concentration of 2560 μM. After a 10-s incubation, the excess H_2O_2 was removed upon the addition of catalase (26 units). At various times, aliquots of the reaction mixture were removed and rapidly quenched with ascorbate, as described under "Experimental Procedures."

SwMb concentration	Cross-linked products[a]		
	1 min	5 min	10 h
μM	%	%	%
10	44 ± 2	44 ± 4	47 ± 5
80	35 ± 6	37 ± 6	47 ± 3
160	36.4 ± 0.7	40 ± 6	51 ± 2
320	42 ± 4	47 ± 2	56 ± 1
640	48 ± 2	52.9 ± 0.9	61.4 ± 0.7
1280	53.3 ± 0.8	60.4 ± 0.7	68 ± 1
2560	59 ± 3	67.8 ± 0.5	73 ± 1

[a] The relative amount of cross-linked products formed were calculated by deconvolution of the FPLC traces as described under "Methods and Materials." The number of Gaussian peaks contained in each chromatograph was fixed to 5.

does not detectably alter the heme environment. In agreement with this, HPLC analysis indicates that under our experimental conditions, no more than 2% of the heme became covalently bound to the protein. Previous studies have shown that covalent heme binding is only quantitatively significant at lower pH values (43).

The recovered monomer after reduction to the ferric state is converted by H_2O_2 to dimers and trimers to the same extent as native SwMb. Similar treatment of the dimer resulted in formation of the trimer and tetramer due to a second round of oligomerization, but interestingly also produced a significant amount of monomeric product. Proteolytic digestion of the recovered monomer and dimer showed that 47% of the tyrosines were lost in the dimer and 14% in the recovered monomer. The dimer fraction contained dityrosine cross-links, as previously reported (16), but was found to also have isodityrosine cross-links. Isodityrosine accounted for 15.2% of the lost tyrosines, and dityrosine accounted for 6.8%. The isodityrosine was missed in earlier experiments because it does not fluoresce and thus is more difficult to detect (16). The fate of the other 25% of the tyrosines that were lost is not known, but this loss does not result from degradation of dityrosine and isodityrosine during the work-up and analysis procedures. No dityrosine and isodityrosine were detected in the recovered monomer, although 14% of the tyrosine content was still lost. The tyrosines clearly suffer fates other than simple conversion to dityrosine or isodityrosine cross-links.

Reaction of SwMb with H_2O_2 converts the ferric to the ferryl state without the formation of spectroscopically observable intermediates (Fig. 1). The protein is concurrently converted to dimeric and trimeric products. A direct correlation is observed between the extent of ferryl formation as a function of the equivalents of H_2O_2 and the amount of oligomeric products formed (Fig. 2). Extrapolation of the data indicates that maximum ferryl formation requires a single equivalent of H_2O_2 and that maximal oligomer formation requires only a slightly higher amount (1.4 eq). However, even with the optimal concentration of H_2O_2, the oligomeric products accounted for only ~60% of the total protein. The other 40% of the protein remained monomeric. Kinetic simulations of the *curves* in Fig. 2 suggest that the accumulation of ferryl Mb is not complete, because ~36% of the ferryl species that is produced is reduced to the ferric state during the titration. Furthermore, at a fixed H_2O_2/Mb ratio of 1, the yield of oligomeric products increases as the protein concentration increases (Fig. 3). At higher protein concentrations, the monomer and trimer are partially converted into a tetrameric product. An estimate of the number of oxidation equivalents consumed in forming the oligomeric products, based on the assumption that the proteins are held together by dityrosine or isodityrosine cross-links (Table I), indicates that oligomerization consumes from 30 to 46% of the added oxidizing equivalents as the protein concentration rises from 40 to 2560 μM. The increase in oligomeric products with protein concentration is expected, since the formation of dityrosine or isodityrosine bonds requires the collision of two tyrosyl radicals. If the tyrosyl radicals are transient, the higher their concentration, the higher the expected yield of oligomers.

After reduction to the ferric state, the oligomerization-resistant monomer recovered from incubations of SwMb with H_2O_2 forms the same oligomeric products as the original native protein upon retreatment with H_2O_2. A smooth autoreduction of the ferryl to the ferric species is spectroscopically observed if the monomer is rapidly recovered from the reaction of SwMb with H_2O_2 (Fig. 8). If the recovered protein is again treated with H_2O_2, an inverse relationship is observed between the fraction of the protein in the ferryl (*versus* ferric) state and the yield of oligomerization products. This quantitative relationship indicates that the ferryl moiety protects the protein from reaction with H_2O_2, but as it reverts to the ferric state, it is again susceptible to ferryl formation and oligomerization.

At all protein concentrations, the combined yield of oligomeric products decreases as the H_2O_2/Mb ratio rises above 2–3. Two possible explanations for this decrease are that the oligomers are polymerized into undetectable aggregates or that they undergo an oxidative depolymerization. The finding that the decrease in oligomers is paralleled by an increase in the amount of the monomer, together with the failure to detect polymeric products by gel filtration, SDS-PAGE, or precipitation, argues that depolymerization accounts for the bulk of the decrease in the dimer and trimer. The nature of the depolymerization reaction is not known, but rupture of the carbon-carbon bond in a dityrosine cross-link appears unlikely. However, oxidation of an isodityrosine link to a quinone-like structure followed by hydrolytic cleavage of the ether bond provides a plausible mechanism for oligomer depolymerization. Digestion of the monomer recovered from the depolymerization experiments did not result in the detection of significant amounts of modified amino acids, possibly because they are unstable and degrade during the incubation or digestion procedures.

To determine whether the protein radicals that result in oligomerization can be generated by inter- rather than intramolecular transmittal of the unpaired electron density, we incubated apoSwMb together with the heme-containing SwMb Y151F mutant and H_2O_2. Previous studies have shown that Tyr^{151} is absolutely required for protein oligomerization (17), so that the Y151F mutant, despite the presence of a normal heme group, is not able to dimerize. The apoSwMb lacks the redox active metal required to react with H_2O_2 and therefore also is not able to dimerize. Thus, neither protein dimerizes if it is incubated alone with H_2O_2 (Fig. 6). However, if interprotein electron transfer is feasible, incubation of the two proteins should allow protein radicals formed on the Y151F mutant to be transferred to the apoSwMb. Since this protein retains Tyr^{151} and is able to dimerize, the observation that it does, in fact, undergo dimerization provides direct evidence for interprotein transfer of the radical center (Fig. 6). A related experiment was carried out some years ago in which equine MetMb (which lacks Tyr^{151}) was incubated with SwMb reconstituted with zinc protoporphyrin IX (15). Dimerization of the modified

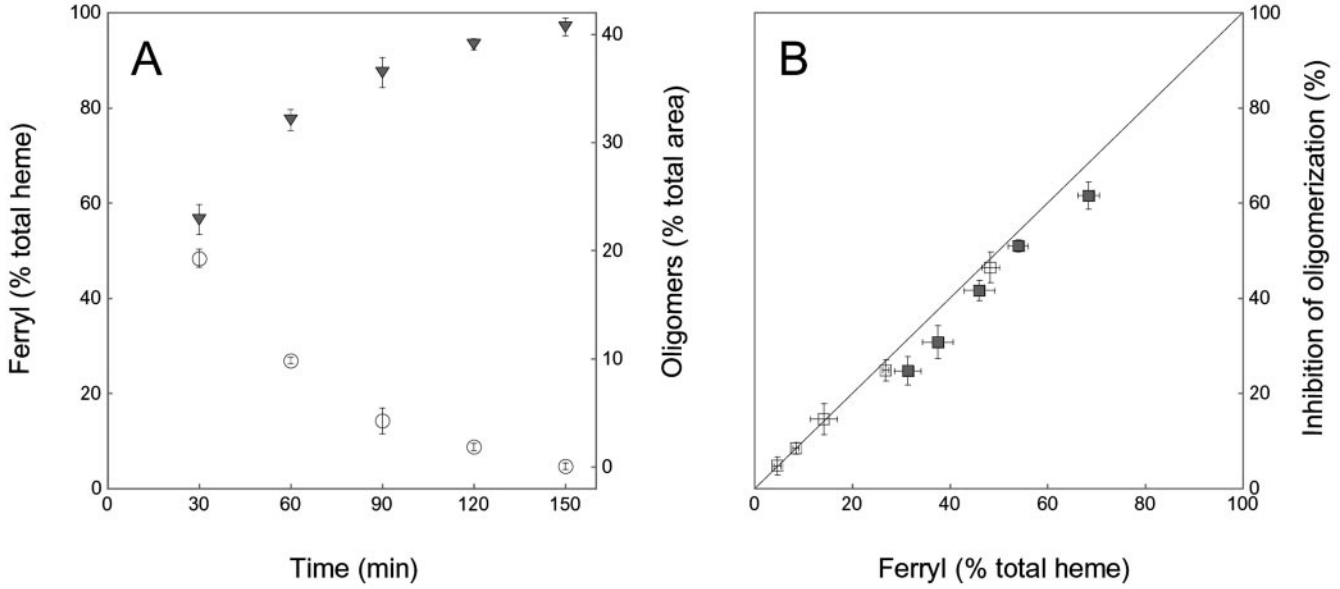

FIG. 8. **Autoreduction of monomeric form of H_2O_2-treated Mb and capacity to oligomerize when reexposed to H_2O_2.** ○, ferryl form (percentage of total heme); ▼, oligomerization yield (percentage of total area); ■, pH 6.8; □, pH 8.0.

protein was not observed in those experiments. The salient differences between these two experiments are the earlier use of horse Mb instead of the SwMb Y151F mutant as the non-dimerizable but redox-active protein and the use of apoSwMb reconstituted with zinc protoporphyrin instead of apoSwMb as the radical acceptor. It is possible that radical transfer between horse Mb and SwMb is less favored than between SwMb and its Y151F mutant or that the higher flexibility of apoSwMb than zinc-containing horse Mb facilitates the electron transfer. In any case, the present evidence provides direct, unambiguous evidence for interprotein radical transfer.

The ferryl species formed in the reaction of SwMb with H_2O_2 is slowly reduced back to the ferric state, although the spectrum of the final protein differs slightly from that of the original met-SwMb (Fig. 7*A*). The autoreduction occurs in at least two phases, a rapid phase with $t = 3.4$ min and a slower phase with $t = 25.9$ min. At relatively low protein concentrations, the autoreduction rates are independent of protein concentration, indicating that the electron employed in the reduction is delivered intramolecularly. However, at higher protein concentrations, the oligomerization is enhanced, which decreases the lifetime of the ferryl species. Analysis of the oligomeric products shows that most of the oligomers are formed very quickly in the initial reaction, but oligomeric product formation continues in parallel with autoreduction of the ferryl species. Thus, slow electron transfer to the ferryl species produces the tyrosine radicals required for dimer and trimer formation. This is a particularly well defined process in that, unlike the initial reaction in which the oxidizing species could theoretically be either the ferryl porphyrin radical cation or a hydroxyl radical, in the second reaction the oxidizing species is unambiguously the ferryl moiety. The kinetic results clearly demonstrate that an electron can be transferred intramolecularly from Tyr^{151} to the iron, either directly or via intervening radical species. Furthermore, at higher protein concentrations, an electron can also be transferred from the tyrosine of one protein to the ferryl species of another, presumably by a direct process that measurably accelerates the rate of ferryl autoreduction.

REFERENCES

1. Sivaraja, M., Goodin, D. B., Smith, M., and Hoffman, B. M. (1989) *Science* **245,** 738–740
2. Tsai, A., Wu, G., Palmer, G., Bambai, B., Koehn, J. A., Marshall, P. J., and Kulmacz, R. J. (1999) *J. Biol. Chem.* **274,** 21695–21700
3. Shalin, M., Petersson, L., Graslund, A., Ehrenberg, A., Sjöberg, B.-M., and Thelander, L. (1987) *Biochemistry* **26,** 5541–5548
4. Volker Wagner, A. F., Frey, M., Neugebauer, F. A., Schäfer, W., and Knappe, J. (1992) *Proc. Natl. Acad. Sci. U. S. A.* **89,** 996–1000
5. Whittaker, M. M., and Whittaker, J. W. (1990) *J. Biol. Chem.* **265,** 9610–9613
6. Blodig, W., Smith, A. T., Doyle, W. A., and Piontek, K. (2001) *J. Mol. Biol.* **305,** 851–861
7. Dorlet, P., Seibold, S. A., Babcock, G. T., Gerfen, G. J., Smith, W. L., Tsai, A. L., and Un, S. (2002) *Biochemistry* **41,** 6107–6114
8. Qian, S. Y., Chen, Y. R., Deterding, L. J., Fann, Y. C., Chignell, C. F., Tomer, K. B., and Mason, R. P. (2002) *Biochem. J.* **363,** 281–288
9. Rich, P. R., Rigby, S. E., and Heathcote, P. (2002) *Biochim. Biophys. Acta* **1554,** 137–146
10. Yonetani, T., and Schleyer, H. (1967) *J. Biol. Chem.* **242,** 1974–1979
11. Ivancich, A., Jouve, H. M., Sartor, B., and Gaillard, J. (1997) *Biochemistry* **36,** 9356–9364
12. King, N. K., and Winfield, M. E. (1963) *J. Biol. Chem.* **238,** 1520–1528
13. Miki, H., Harada, K., Yamazaki, I., Tamura, M., and Watanabe, H. (1989) *Arch. Biochem. Biophys.* **275,** 354–362
14. King, N. K., Looney, F. D., and Winfield, M. E. (1967) *Biochim. Biophys. Acta* **133,** 65–82
15. Tew, D., and Ortiz de Montellano, P. R. (1988) *J. Biol. Chem.* **263,** 17880–17886
16. Catalano, C. E., Choe, Y. S., and Ortiz de Montellano, P. R. (1989) *J. Biol. Chem.* **264,** 10534–10541
17. Wilks, A., and Ortiz de Montellano, P. R. (1992) *J. Biol. Chem.* **267,** 8827–8833
18. Rao, S., Wilks, A., and Ortiz de Montellano, P. R. (1993) *J. Biol. Chem.* **268,** 803–809
19. Fancy, D., and Kodadek, T. (1998) *Biochem. Biophys. Res. Commun.* **247,** 420–426
20. Garrison, W. M. (1987) *Chem. Rev.* **87,** 381–398
21. Davies, M. J., Fu, S., Wang, H., and Dean, R. T. (1999) *Free Radic. Biol. Med.* **27,** 1151–1163
22. Foerder, C. A., and Shapiro, B. M. (1977) *Proc. Natl. Acad. Sci. U. S. A.* **74,** 4214–4218
23. Stadtman, E. R., and Berlett, B. S. (1997) *Chem. Res. Toxicol.* **10,** 485–494
24. Degray J. A., Gunther, M. R., Tschirret-Guth, R., Ortiz de Montellano, P. R., and Mason, R. P. (1997) *J. Biol. Chem.* **272,** 2359–2362
25. Witting, P. K., Douglas, D. J., and Mauk, A. G. (2000) *J. Biol. Chem.* **275,** 20391–20398
26. Fenwick, C. W., and English, A. M. (1996) *J. Am. Chem. Soc.* **118,** 12236–12237
27. Matsui, T., Ozaki, S., and Watanabe, Y. (1999) *J. Am. Chem. Soc.* **121,** 9952–9957
28. Egawa, T., Shimada, H., and Ishimura, Y. (2000) *J. Biol. Chem.* **275,** 34858–34866
29. Thomas, E. L. (1985) in *The Lactoperoxidase System: Chemistry and Biological Significance* (Pruitt, K. M., and Tenovuo, J. O., eds) pp. 31–54, Marcel Dekker, New York
30. Dunford, H. B. (1999) *Heme Peroxidases*, p. 20, Wiley-VCH, New York
31. Courtin, F., Michot, J.-L., Virion, A., Pommier, J., and Deme, D. (1984) *Biochem. Biophys. Res. Commun.* **121,** 463–470
32. Lardinois, O. M., Medzihradszky, K. F., and Ortiz de Montellano, P. R. (1999) *J. Biol. Chem.* **274,** 35441–35448
33. Colas, C., Kuo, J. M., and Ortiz de Montellano, P. R. (2002) *J. Biol. Chem.* **277,** 7191–7200
34. Lardinois, O. M., and Ortiz de Montellano, P. R. (2001) *J. Biol. Chem.* **276,** 23186–23191
35. Antonini, E., and Brunori, M. (1971) *Hemoglobin and Myoglobin in Their*

Reactions with Ligands, p. 44, Elsevier, New York
36. Goto, Y., Calciano, L. J., and Fink, A. L. (1990) *Proc. Natl. Acad. Sci. U. S. A.* **87,** 573–577
37. Nelson, D. P., and Kiesow, L. A. (1972) *Anal. Biochem.* **49,** 474–478
38. Fry, S. C. (1984) *Methods Enzymol.* **107,** 388–397
39. Jacob, J. S., Cistola, D. P., Hsu, F. F., Muzaffar, S., Mueller D. M., Hazen, S. L., and Heinecke, J. W. (1996) *J. Biol. Chem.* **271,** 19950–19956
40. Satake, K., Okuyama, T., Ohashi, M., and Shinoda, T. (1960) *J. Biochem.* (*Tokyo*) **47,** 654–660
41. LeBrun, L., Hoch, U., and Ortiz de Montellano, P. R. (2002) *J. Biol. Chem.* **277,** 12755–12761
42. Garner, M. H., Garner, W. H., and Gurd, F. R. N. (1973) *J. Biol. Chem.* **249,** 1513–1518
43. Reeder, B. J., Svistunenko, D. A., Sharpe, M. A., and Wilson, M. T. (2002) *Biochemistry* **41,** 367–375
44. Gibson, J. F., Ingram, D. J. E., and Nicholls, P. (1958) *Nature* **181,** 1398–1399
45. Svistunenko, D. A., Dunne, J., Fryer, M., Nicholls, P., Reeder, B. J., Wilson, M. T., Bigotti, M. G., Cutruzzola, F., and Cooper, C. E. (2002) *Biophys. J.* **83,** 2845–2855

Protein Synthesis, Post-Translation Modification, and Degradation:

Intra- and Intermolecular Transfers of Protein Radicals in the Reactions of Sperm Whale Myoglobin with Hydrogen Peroxide

Olivier M. Lardinois and Paul R. Ortiz de Montellano

J. Biol. Chem. 2003, 278:36214-36226.
doi: 10.1074/jbc.M304726200 originally published online July 10, 2003